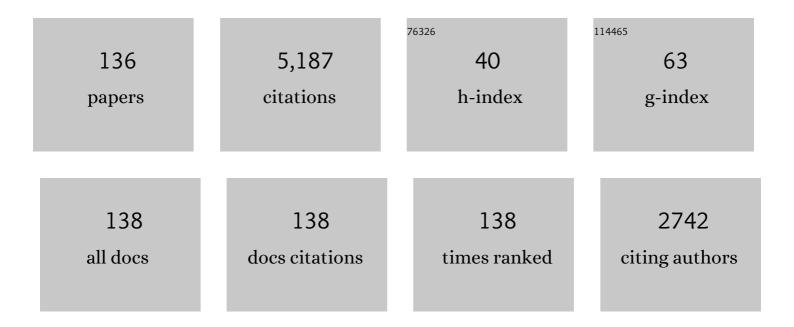
## Li-Xin Chen

List of Publications by Year in descending order

Source: https://exaly.com/author-pdf/7000956/publications.pdf Version: 2024-02-01



#	Article	IF	CITATIONS
1	All-temperature batteries enabled by fluorinated electrolytes with non-polar solvents. Nature Energy, 2019, 4, 882-890.	39.5	557
2	Critical Review on Lowâ€Temperature Liâ€Ion/Metal Batteries. Advanced Materials, 2022, 34, e2107899.	21.0	204
3	Novel 1D carbon nanotubes uniformly wrapped nanoscale MgH2 for efficient hydrogen storage cycling performances with extreme high gravimetric and volumetric capacities. Nano Energy, 2019, 61, 540-549.	16.0	124
4	A striking catalytic effect of facile synthesized ZrMn <sub>2</sub> nanoparticles on the de/rehydrogenation properties of MgH <sub>2</sub> . Journal of Materials Chemistry A, 2019, 7, 5626-5634.	10.3	118
5	Achieving superior hydrogen storage properties of MgH2 by the effect of TiFe and carbon nanotubes. Chemical Engineering Journal, 2021, 422, 130101.	12.7	116
6	ZIF-67 derived Co@CNTs nanoparticles: Remarkably improved hydrogen storage properties of MgH2 and synergetic catalysis mechanism. International Journal of Hydrogen Energy, 2019, 44, 1059-1069.	7.1	111
7	Anion–Diluent Pairing for Stable High-Energy Li Metal Batteries. ACS Energy Letters, 2022, 7, 1338-1347.	17.4	108
8	Facile synthesized Fe nanosheets as superior active catalyst for hydrogen storage in MgH2. International Journal of Hydrogen Energy, 2019, 44, 21955-21964.	7.1	100
9	Enhanced hydrogen storage properties of MgH <sub>2</sub> with numerous hydrogen diffusion channels provided by Na <sub>2</sub> Ti <sub>3</sub> O <sub>7</sub> nanotubes. Journal of Materials Chemistry A, 2017, 5, 6178-6185.	10.3	89
10	Excellent catalysis of TiO <sub>2</sub> nanosheets with high-surface-energy {001} facets on the hydrogen storage properties of MgH <sub>2</sub> . Nanoscale, 2019, 11, 7465-7473.	5.6	89
11	Facile synthesis of Co/Pd supported by few-walled carbon nanotubes as an efficient bidirectional catalyst for improving the low temperature hydrogen storage properties of magnesium hydride. Journal of Materials Chemistry A, 2019, 7, 5277-5287.	10.3	88
12	Superior de/hydrogenation performances of MgH2 catalyzed by 3D flower-like TiO2@C nanostructures. Journal of Energy Chemistry, 2020, 46, 191-198.	12.9	88
13	Transition metal (Co, Ni) nanoparticles wrapped with carbon and their superior catalytic activities for the reversible hydrogen storage of magnesium hydride. Physical Chemistry Chemical Physics, 2017, 19, 4019-4029.	2.8	86
14	Novel AgPd hollow spheres anchored on graphene as an efficient catalyst for dehydrogenation of formic acid at room temperature. Journal of Materials Chemistry A, 2016, 4, 657-666.	10.3	75
15	Remarkably Improved Hydrogen Storage Performance of MgH <sub>2</sub> Catalyzed by Multivalence NbH <sub><i>x</i></sub> Nanoparticles. Journal of Physical Chemistry C, 2015, 119, 8554-8562.	3.1	73
16	Finite element modeling of piezoresponse in nanostructured ferroelectric films. Applied Physics Letters, 2004, 84, 2626-2628.	3.3	70
17	Development of Ti–Cr–Mn–Fe based alloys with high hydrogenÂdesorption pressures for hybrid hydrogen storage vessel application. International Journal of Hydrogen Energy, 2013, 38, 12803-12810.	7.1	61
18	Synergistic Catalytic Activity of Porous Rod-like TMTiO <sub>3</sub> (TM = Ni and Co) for Reversible Hydrogen Storage of Magnesium Hydride. Journal of Physical Chemistry C, 2018, 122, 27973-27982.	3.1	61

#	Article	IF	CITATIONS
19	Excellent synergistic catalytic mechanism of in-situ formed nanosized Mg2Ni and multiple valence titanium for improved hydrogen desorption properties of magnesium hydride. International Journal of Hydrogen Energy, 2019, 44, 1750-1759.	7.1	61
20	Enhanced hydrogen storage capacity and reversibility of LiBH4 nanoconfined in the densified zeolite-templated carbon with high mechanical stability. Nano Energy, 2015, 15, 244-255.	16.0	58
21	Highly synergetic catalytic mechanism of Ni@g-C3N4 on the superior hydrogen storage performance of Li-Mg-B-H system. Energy Storage Materials, 2018, 13, 199-206.	18.0	58
22	Two-dimensional ZrCo nanosheets as highly effective catalyst for hydrogen storage in MgH2. Journal of Alloys and Compounds, 2019, 805, 295-302.	5.5	57
23	Synergistic catalysis in monodispersed transition metal oxide nanoparticles anchored on amorphous carbon for excellent low-temperature dehydrogenation of magnesium hydride. Materials Today Energy, 2019, 12, 146-154.	4.7	57
24	Optically active threeâ€dimensionally confined structures realized via molecular beam epitaxical growth on nonplanar GaAs (111)B. Applied Physics Letters, 1993, 63, 2905-2907.	3.3	56
25	Non-noble trimetallic Cu-Ni-Co nanoparticles supported on metal-organic frameworks as highly efficient catalysts for hydrolysis of ammonia borane. Journal of Alloys and Compounds, 2018, 741, 501-508.	5.5	55
26	Effect of rare earth doping on the hydrogen storage performance of Ti1.02Cr1.1Mn0.3Fe0.6 alloy for hybrid hydrogen storage application. Journal of Alloys and Compounds, 2018, 731, 524-530.	5.5	55
27	Active species of CeAl4 in the CeCl3-doped sodium aluminium hydride and its enhancement on reversible hydrogen storage performance. Chemical Communications, 2009, , 6857.	4.1	54
28	Remarkable hydrogen desorption properties and mechanisms of the Mg <sub>2</sub> FeH <sub>6</sub> @MgH <sub>2</sub> core–shell nanostructure. Journal of Materials Chemistry A, 2015, 3, 5517-5524.	10.3	54
29	Enhanced hydriding–dehydriding performance of 2LiBH4–MgH2 composite by the catalytic effects of transition metal chlorides. Journal of Materials Chemistry, 2012, 22, 20764.	6.7	53
30	Low-Temperature Reversible Hydrogen Storage Properties of LiBH <sub>4</sub> : A Synergetic Effect of Nanoconfinement and Nanocatalysis. Journal of Physical Chemistry C, 2014, 118, 11252-11260.	3.1	51
31	High catalytic efficiency of amorphous TiB2 and NbB2 nanoparticles for hydrogen storage using the 2LiBH4–MgH2 system. Journal of Materials Chemistry A, 2013, 1, 11368.	10.3	47
32	Influence of Ti super-stoichiometry on the hydrogen storage properties of Ti1+xCr1.2Mn0.2Fe0.6 (x=0–0.1) alloys for hybrid hydrogen storage application. Journal of Alloys and Compounds, 2014, 585, 307-311.	5.5	47
33	Enhanced hydrogen storage properties of MgH2 by the synergetic catalysis of Zr0.4Ti0.6Co nanosheets and carbon nanotubes. Applied Surface Science, 2020, 504, 144465.	6.1	47
34	Catalytic Mechanism of New TiC-Doped Sodium Alanate for Hydrogen Storage. Journal of Physical Chemistry C, 2009, 113, 20745-20751.	3.1	46
35	Improvement on the kinetic and thermodynamic characteristics of Zr1-xNbxCo (xÂ= 0–0.2) alloys for hydrogen isotope storage and delivery. Journal of Alloys and Compounds, 2019, 784, 1062-1070.	5.5	46
36	The remarkably improved hydrogen storage performance of MgH <sub>2</sub> by the synergetic effect of an FeNi/rGO nanocomposite. Dalton Transactions, 2020, 49, 4146-4154.	3.3	46

#	Article	IF	CITATIONS
37	Effects of NbF5 addition on the de/rehydrogenation properties of 2LiBH4/MgH2 hydrogen storage system. International Journal of Hydrogen Energy, 2012, 37, 13147-13154.	7.1	45
38	Self-templated carbon enhancing catalytic effect of ZrO2 nanoparticles on the excellent dehydrogenation kinetics of MgH2. Carbon, 2020, 166, 46-55.	10.3	45
39	Superior catalytic effects of FeCo nanosheets on MgH <sub>2</sub> for hydrogen storage. Dalton Transactions, 2019, 48, 12699-12706.	3.3	43
40	Effects of fluoride additives on dehydrogenation behaviors of 2LiBH4Â+ÂMgH2 system. International Journal of Hydrogen Energy, 2012, 37, 1021-1026.	7.1	41
41	A self-purifying electrolyte enables high energy Li ion batteries. Energy and Environmental Science, 2022, 15, 3331-3342.	30.8	40
42	Size effect on hydrogen storage properties of NaAlH4 confined in uniform porous carbons. Nano Energy, 2013, 2, 995-1003.	16.0	38
43	Orientation dependence of the converse piezoelectric constantsfor epitaxial single domain ferroelectric films. Applied Physics Letters, 2004, 85, 278-280.	3.3	37
44	A new strategy for remarkably improving anti-disproportionation performance and cycling stabilities of ZrCo-based hydrogen isotope storage alloys by Cu substitution and controlling cutoff desorption pressure. International Journal of Hydrogen Energy, 2019, 44, 28242-28251.	7.1	36
45	Effect of Mn substitution for Co on the structural, kinetic, and thermodynamic characteristics of ZrCo1ⰒMn (x=0–0.1) alloys for tritium storage. International Journal of Hydrogen Energy, 2017, 42, 28498-28506.	7.1	35
46	Synergistic Effect of LiBH <sub>4</sub> and LiAlH <sub>4</sub> Additives on Improved Hydrogen Storage Properties of Unexpected High Capacity Magnesium Hydride. Journal of Physical Chemistry C, 2018, 122, 2528-2538.	3.1	35
47	Excellent catalysis of Mn <sub>3</sub> O <sub>4</sub> nanoparticles on the hydrogen storage properties of MgH <sub>2</sub> : an experimental and theoretical study. Nanoscale Advances, 2020, 2, 1666-1675.	4.6	35
48	Enhanced low temperature hydrogen desorption properties and mechanism of Mg(BH4)2 composited with 2D MXene. International Journal of Hydrogen Energy, 2019, 44, 24292-24300.	7.1	34
49	An in-depth study on the thermodynamics and kinetics of disproportionation behavior in ZrCo–H systems. Journal of Materials Chemistry A, 2020, 8, 9322-9330.	10.3	34
50	Investigation on Ti–Zr–Cr–Fe–V based alloys for metal hydride hydrogen compressor at moderate working temperatures. International Journal of Hydrogen Energy, 2021, 46, 21580-21589.	7.1	34
51	AuPd Nanoparticles Anchored on Nitrogen-Decorated Carbon Nanosheets with Highly Efficient and Selective Catalysis for the Dehydrogenation of Formic Acid. Journal of Physical Chemistry C, 2018, 122, 4792-4801.	3.1	33
52	Hydriding-dehydriding kinetics and the microstructure of La- and Sm-doped NaAlH4 prepared via direct synthesis method. International Journal of Hydrogen Energy, 2011, 36, 10861-10869.	7.1	32
53	Development of Ti-Zr-Mn-Cr-V based alloys for high-density hydrogen storage. Journal of Alloys and Compounds, 2021, 875, 160035.	5.5	32
54	Mn nanoparticles enhanced dehydrogenation and hydrogenation kinetics of MgH2 for hydrogen storage. Transactions of Nonferrous Metals Society of China, 2021, 31, 3469-3477.	4.2	31

#	Article	IF	CITATIONS
55	Microstructure and hydrogen storage characteristics of nanocrystalline Mg+xwt% LaMg2Ni (x=0–30) composites. International Journal of Hydrogen Energy, 2010, 35, 2786-2790.	7.1	29
56	Highly dispersed metal nanoparticles on TiO2 acted as nano redox reactor and its synergistic catalysis on the hydrogen storage properties of magnesium hydride. International Journal of Hydrogen Energy, 2019, 44, 15100-15109.	7.1	29
57	Metal organic framework supported niobium pentoxide nanoparticles with exceptional catalytic effect on hydrogen storage behavior of MgH2. Green Energy and Environment, 2023, 8, 589-600.	8.7	29
58	Realization of three-dimensionally confined structures via one-step in situ molecular beam epitaxy on appropriately patterned GaAs(111)B and GaAs(001). Journal of Vacuum Science & Technology an Official Journal of the American Vacuum Society B, Microelectronics Processing and Phenomena, 1994, 12, 1071.	1.6	28
59	The hydrogen storage properties and microstructure of Ti-doped sodium aluminum hydride prepared by ball-milling. International Journal of Hydrogen Energy, 2007, 32, 2475-2479.	7.1	28
60	Enhanced hydriding–dehydriding performance of a 2LiH–MgB2 composite by the catalytic effects of Ni–B nanoparticles. Journal of Materials Chemistry A, 2013, 1, 10184.	10.3	28
61	Enhanced hydrogen storage properties of LiBH4 modified by NbF5. International Journal of Hydrogen Energy, 2014, 39, 11675-11682.	7.1	28
62	Facile synthesis of bowl-like 3D Mg(BH <sub>4</sub> ) <sub>2</sub> –NaBH <sub>4</sub> –fluorographene composite with unexpected superior dehydrogenation performances. Journal of Materials Chemistry A, 2017, 5, 9723-9732.	10.3	28
63	In-situ synthesis of amorphous Mg(BH4)2 and chloride composite modified by NbF5 for superior reversible hydrogen storage properties. International Journal of Hydrogen Energy, 2020, 45, 2044-2053.	7.1	28
64	Extreme high reversible capacity with over 8.0Âwt% and excellent hydrogen storage properties of MgH2 combined with LiBH4 and Li3AlH6. Journal of Energy Chemistry, 2020, 50, 296-306.	12.9	28
65	Tuning electrolyte enables microsized Sn as an advanced anode for Li-ion batteries. Journal of Materials Chemistry A, 2021, 9, 1812-1821.	10.3	28
66	Fluorographene nanosheets enhanced hydrogen absorption and desorption performances of magnesium hydride. International Journal of Hydrogen Energy, 2014, 39, 12715-12726.	7.1	26
67	Highly efficient ZrH2 nanocatalyst for the superior hydrogenation kinetics of magnesium hydride under moderate conditions: Investigation and mechanistic insights. Applied Surface Science, 2021, 541, 148375.	6.1	26
68	Effect of 90° domain movement on the piezoelectric response of patterned PbZr0.2Ti0.8O3â^•SrTiO3â^•Si heterostructures. Applied Physics Letters, 2005, 87, 072907.	3.3	25
69	Insights into 2D graphene-like TiO2 (B) nanosheets as highly efficient catalyst for improved low-temperature hydrogen storage properties of MgH2. Materials Today Energy, 2020, 16, 100411.	4.7	25
70	Enhanced hydrogen storage properties of high-loading nanoconfined LiBH4–Mg(BH4)2 composites with porous hollow carbon nanospheres. International Journal of Hydrogen Energy, 2021, 46, 852-864.	7.1	25
71	Mitigating irreversible capacity loss for higher-energy lithium batteries. Energy Storage Materials, 2022, 48, 44-73.	18.0	25
72	Enhanced hydrogen desorption properties of LiBH4–Ca(BH4)2 by a synergetic effect of nanoconfinement and catalysis. International Journal of Hydrogen Energy, 2016, 41, 17462-17470.	7.1	24

#	Article	IF	CITATIONS
73	Building robust architectures of carbon-wrapped transition metal nanoparticles for high catalytic enhancement of the 2LiBH <sub>4</sub> -MgH <sub>2</sub> system for hydrogen storage cycling performance. Nanoscale, 2016, 8, 14898-14908.	5.6	24
74	Study on low-vanadium Ti–Zr–Mn–Cr–V based alloys for high-density hydrogen storage. International Journal of Hydrogen Energy, 2022, 47, 1710-1722.	7.1	24
75	Unraveling the degradation mechanism for the hydrogen storage property of Fe nanocatalyst-modified MgH <sub>2</sub> . Inorganic Chemistry Frontiers, 2022, 9, 3874-3884.	6.0	24
76	Thermodynamics, Kinetics, and Modeling Investigation on the Dehydrogenation of CeAl <sub>4</sub> -Doped NaAlH <sub>4</sub> Hydrogen Storage Material. Journal of Physical Chemistry C, 2011, 115, 22680-22687.	3.1	23
77	Study on the dehydrogenation properties and reversibility of Mg(BH4)2AlH3 composite under moderate conditions. International Journal of Hydrogen Energy, 2017, 42, 8050-8056.	7.1	23
78	Remarkable enhancement in dehydrogenation properties of Mg(BH4)2 modified by the synergetic effect of fluorographite and LiBH4. International Journal of Hydrogen Energy, 2015, 40, 14163-14172.	7.1	22
79	Influence of Fe content on the microstructure and hydrogen storage properties of Ti16Zr5Cr22V57â^'xFex (x=2–8) alloys. International Journal of Hydrogen Energy, 2010, 35, 8143-8148.	7.1	21
80	Fast hydrogen release under moderate conditions from NaBH <sub>4</sub> destabilized by fluorographite. RSC Advances, 2013, 4, 2550-2556.	3.6	21
81	Ternary perovskite nickel titanate/reduced graphene oxide nano-composite with improved lithium storage properties. RSC Advances, 2016, 6, 61312-61318.	3.6	21
82	La2O3-modified highly dispersed AuPd alloy nanoparticles and their superior catalysis on the dehydrogenation of formic acid. International Journal of Hydrogen Energy, 2017, 42, 9353-9360.	7.1	21
83	Remarkably improved hydrogen storage properties of carbon layers covered nanocrystalline Mg with certain air stability. International Journal of Hydrogen Energy, 2020, 45, 28134-28143.	7.1	20
84	The dehydrogenation kinetics and reversibility improvements of Mg(BH4)2 doped with Ti nano-particles under mild conditions. International Journal of Hydrogen Energy, 2021, 46, 23737-23747.	7.1	20
85	Superior dehydrogenation performance of nanoscale lithium borohydride modified with fluorographite. International Journal of Hydrogen Energy, 2014, 39, 896-904.	7.1	19
86	Influence of annealing treatment on the microstructure and hydrogen storage performance of Ti1.02Cr1.1Mn0.3Fe0.6 alloy for hybrid hydrogen storage application. Journal of Alloys and Compounds, 2015, 636, 117-123.	5.5	19
87	Superior catalysis of NbN nanoparticles with intrinsic multiple valence on reversible hydrogen storage properties of magnesium hydride. International Journal of Hydrogen Energy, 2021, 46, 814-822.	7.1	19
88	0D/1D/2D Co@Co2Mo3O8 nanocomposite constructed by mutual-supported Co2Mo3O8 nanosheet and Co nanoparticle: Synthesis and enhanced hydrolytic dehydrogenation of ammonia borane. Chemical Engineering Journal, 2022, 431, 133697.	12.7	19
89	Ultrahigh reversible hydrogen capacity and synergetic mechanism of 2LiBH4-MgH2 system catalyzed by dual-metal fluoride. Chemical Engineering Journal, 2022, 433, 134482.	12.7	19
90	Formation mechanism of MgB2 in 2LiBH4 + MgH2 system for reversible hydrogen storage. Transactions of Nonferrous Metals Society of China, 2011, 21, 1040-1046.	4.2	18

#	Article	IF	CITATIONS
91	Superior Reversible Hydrogen Storage Properties and Mechanism of LiBH <sub>4</sub> –MgH <sub>2</sub> –Al Doped with NbF <sub>5</sub> Additive. Journal of Physical Chemistry C, 2018, 122, 7613-7620.	3.1	18
92	Study on the modification of Zr-Mn-V based alloys for hydrogen isotopes storage and delivery. Journal of Alloys and Compounds, 2019, 797, 185-193.	5.5	18
93	PdCoNi nanoparticles supported on nitrogen-doped porous carbon nanosheets for room temperature dehydrogenation of formic acid. International Journal of Hydrogen Energy, 2019, 44, 11675-11683.	7.1	18
94	LiAlH <sub>4</sub> as a "Microlighter―on the Fluorographite Surface Triggering the Dehydrogenation of Mg(BH <sub>4</sub> ) <sub>2</sub> : Toward More than 7 wt % Hydrogen Release below 70 °C. ACS Applied Energy Materials, 2020, 3, 3033-3041.	5.1	18
95	Achieving excellent cycle stability in Zr–Nb–Co–Ni based hydrogen isotope storage alloys by controllable phase transformation reaction. Renewable Energy, 2022, 187, 500-507.	8.9	18
96	Grain-to-Grain Stress Interactions in an Electrodeposited Iron Coating. Advanced Materials, 2005, 17, 1221-1226.	21.0	17
97	Extended finite element method coupled with faceâ€based strain smoothing technique for threeâ€dimensional fracture problems. International Journal for Numerical Methods in Engineering, 2015, 102, 1894-1916.	2.8	17
98	The functioning mechanism of Al valid substitution for Co in improving the cycling performance of Zr–Co–Al based hydrogen isotope storage alloys. Journal of Alloys and Compounds, 2020, 848, 156618.	5.5	17
99	Heterostructured Ni/NiO Nanoparticles on 1D Porous MoO <sub><i>x</i></sub> for Hydrolysis of Ammonia Borane. ACS Applied Energy Materials, 2021, 4, 1208-1217.	5.1	17
100	Influence of temperature and hydrogen pressure on the hydriding/dehydriding behavior of Ti-doped sodium aluminum hydride. International Journal of Hydrogen Energy, 2007, 32, 3954-3958.	7.1	16
101	The effect of Cr content on the structural and hydrogen storage characteristics of Ti10V80â^'xFe6Zr4Crx (x=0–14) alloys. Journal of Alloys and Compounds, 2010, 493, 396-400.	5.5	16
102	Comprehensive hydrogen storage properties and catalytic mechanism studies of 2LiBH4–MgH2 system with NbF5 in various addition amounts. International Journal of Hydrogen Energy, 2014, 39, 7050-7059.	7.1	16
103	Dual-Ion Substitution-Induced Unique Electronic Modulation to Stabilize an Orthorhombic Lattice towards Reversible Hydrogen Isotope Storage. ACS Sustainable Chemistry and Engineering, 2021, 9, 9139-9148.	6.7	16
104	Probing an intermediate state by X-ray absorption near-edge structure in nickel-doped 2LiBH4–MgH2 reactive hydride composite at moderate temperature. Materials Today Nano, 2020, 12, 100090.	4.6	15
105	Improved reversible dehydrogenation properties of Mg(BH4)2 catalyzed by dual-cation transition metal fluorides K2TiF6 and K2NbF7. Chemical Engineering Journal, 2021, 412, 128738.	12.7	15
106	Enhanced reversible hydrogen desorption properties and mechanism of Mg(BH4)2-AlH3-LiH composite. Journal of Alloys and Compounds, 2018, 762, 548-554.	5.5	14
107	Facile synthesis of AuPd nanoparticles anchored on TiO2 nanosheets for efficient dehydrogenation of formic acid. Nanotechnology, 2018, 29, 335402.	2.6	14
108	Synergetic Effect of in Situ Formed Nano NbH and LiH <sub>1–<i>x</i></sub> F <sub><i>x</i></sub> for Improving Reversible Hydrogen Storage Properties of the Li–Mg–B–H System. Journal of Physical Chemistry C, 2013, 117, 12019-12025.	3.1	13

#	Article	IF	CITATIONS
109	Synthesis of nanoscale CeAl4 and its high catalytic efficiency for hydrogen storage of sodium alanate. Rare Metals, 2017, 36, 77-85.	7.1	12
110	Regulating local chemistry in ZrCo-based orthorhombic hydrides via increasing atomic interference for ultra-stable hydrogen isotopes storage. Journal of Energy Chemistry, 2022, 69, 397-405.	12.9	12
111	Dynamically Staged Phase Transformation Mechanism of Co-Containing Rare Earth-Based Metal Hydrides with Unexpected Hysteresis Amelioration. ACS Applied Energy Materials, 2022, 5, 3783-3792.	5.1	12
112	Enhanced hydrogen storage properties of a dual-cation (Li <sup>+</sup> , Mg <sup>2+</sup> ) borohydride and its dehydrogenation mechanism. RSC Advances, 2017, 7, 36852-36859.	3.6	11
113	A dandelion-like amorphous composite catalyst with outstanding performance for sodium borohydride hydrogen generation. International Journal of Hydrogen Energy, 2021, 46, 10809-10818.	7.1	11
114	Studies on Ti-Zr-Cr-Mn-Fe-V based alloys for hydrogen compression under mild thermal conditions of water bath. Journal of Alloys and Compounds, 2022, 892, 162145.	5.5	11
115	Monte Carlo simulation of the percolation in Ag30Ge17Se53 amorphous electrolyte films. Applied Physics Letters, 2009, 95, .	3.3	10
116	Effects of Fluoride Additives on the Hydrogen Storage Performance of 2LiBH <sub>4</sub> –Li <sub>3</sub> AlH <sub>6</sub> Destabilized System. Journal of Physical Chemistry C, 2012, 116, 22226-22230.	3.1	10
117	Enhanced reversible hydrogen storage performance of NbCl5 doped 2LiH–MgB2 composite. International Journal of Hydrogen Energy, 2014, 39, 2132-2141.	7.1	10
118	Development of Ti0.85Zr0.17(Cr-Mn-V)1.3Fe0.7-based Laves phase alloys for thermal hydrogen compression at mild operating temperatures. Rare Metals, 2022, 41, 2588-2594.	7.1	10
119	In-situ formation of ultrafine MgNi3B2 and TiB2 nanoparticles: Heterogeneous nucleating and grain coarsening retardant agents for magnesium borate in Li–Mg–B–H reactive hydride composite. International Journal of Hydrogen Energy, 2019, 44, 27529-27541.	7.1	9
120	Excellent Catalysis of Various TiO2 Dopants with Na0.46TiO2 in Situ Formed on the Enhanced Dehydrogenation Properties of NaMgH3. Journal of Physical Chemistry C, 2019, 123, 22832-22841.	3.1	9
121	An impact of hydrogenation phase transformation mechanism on the cyclic stabilizing behavior of Zr0.8Ti0.2Co alloy for hydrogen isotopeÂhandling. Materials Today Energy, 2020, 18, 100554.	4.7	9
122	Ultra-fast dehydrogenation behavior at low temperature of LiAlH4 modified by fluorographite. International Journal of Hydrogen Energy, 2020, 45, 28123-28133.	7.1	9
123	Positive impacts of tuning lattice on cyclic performance in ZrCo-based hydrogen isotopeÂstorage alloys. Materials Today Energy, 2021, 20, 100645.	4.7	9
124	A Novel Li–Ca–B–H Complex Borohydride: Its Synthesis and Hydrogen Storage Properties. Journal of Physical Chemistry C, 2011, 115, 19986-19993.	3.1	7
125	In situ synthesized SnO2 nanorod/reduced graphene oxide low-dimensional structure for enhanced lithium storage. Nanotechnology, 2018, 29, 105705.	2.6	7
126	3-D flow effects on residence time distribution in screw extruders. AICHE Journal, 1996, 42, 1525-1535.	3.6	6

#	Article	IF	CITATIONS
127	The <00l>-oriented growth of Cu2S films and its switching properties. Journal of Electroceramics, 2009, 22, 87-90.	2.0	6
128	Low-cost batteries based on industrial waste Al–Si microparticles and LiFePO <sub>4</sub> for stationary energy storage. Dalton Transactions, 2021, 50, 8322-8329.	3.3	6
129	Hydrogen desorption from MgH2+NH4Cl/graphene composites at low temperatures. Materials Chemistry and Physics, 2021, 263, 124342.	4.0	6
130	Insights into magnesium borohydride dehydrogenation mechanism from its partial reversibility under moderate conditions. Materials Today Energy, 2020, 18, 100552.	4.7	4
131	FIRST-PRINCIPLES CALCULATION OF THE ELECTRONIC STRUCTURE AND MAGNETISM AT THE GRAPHENE/Ni(111) INTERFACE. International Journal of Modern Physics B, 2011, 25, 2791-2800.	2.0	2
132	Hydrogenation reaction characteristics and properties of its hydrides for magnetic regenerative material HoCu2. Journal of Central South University, 2016, 23, 1564-1568.	3.0	1
133	Effect of Different Amounts of TiF3 on the Reversible Hydrogen Storage Properties of 2LiBH4–Li3AlH6 Composite. Frontiers in Chemistry, 2021, 9, 693302.	3.6	1
134	Devolatilization of Polymer Solutions. International Polymer Processing, 1994, 9, 26-32.	0.5	0
135	Fabrication of Micro- and Nanoscale SiC Structures Using Selective Deposition Processes. Materials Research Society Symposia Proceedings, 2003, 782, 1.	0.1	0
136	The Behavior of Hastelloy®C-2000®Alloy Under Strain-Controlled Fatigue Loading. , 2013, , 240-254.		0